THE COMPANY OF
Biologists

RESEARCH ARTICLE

The transmembrane protein Macroglobulin complement-related is essential for septate junction formation and epithelial barrier function in *Drosophila*

Tilmann Bätz[‡], Dominique Förster[*,‡] and Stefan Luschnig[§]

ABSTRACT

Occluding cell-cell junctions in epithelia form physical barriers that separate different membrane domains, restrict paracellular diffusion and prevent pathogens from spreading across tissues. In invertebrates, these functions are provided by septate junctions (SJs), the functional equivalent of vertebrate tight junctions. How the diverse functions of SJs are integrated and modulated in a multiprotein complex is not clear, and many SJ components are still unknown. Here we report the identification of Macroglobulin complement-related (Mcr), a member of the conserved α-2-macroglobulin (α2M) complement protein family, as a novel SJ-associated protein in *Drosophila*. Whereas α2M complement proteins are generally known as secreted factors that bind to surfaces of pathogens and target them for phagocytic uptake, Mcr represents an unusual α2M protein with a predicted transmembrane domain. We show that Mcr protein localizes to lateral membranes of epithelial cells, where its distribution overlaps with SJs. Several SJ components are required for the correct localization of Mcr. Conversely, Mcr is required in a cell-autonomous fashion for the correct membrane localization of SJ components, indicating that membrane-bound rather than secreted Mcr isoforms are involved in SJ formation. Finally, we show that loss of *Mcr* function leads to morphological, ultrastructural and epithelial barrier defects resembling mutants lacking SJ components. Our results, along with previous findings on the role of Mcr in phagocytosis, suggest that Mcr plays dual roles in epithelial barrier formation and innate immunity. Thus, Mcr represents a novel paradigm for investigating functional links between occluding junction formation and pathogen defense mechanisms.

KEY WORDS: Epithelial barrier, Septate junction, Innate immunity, Thioester proteins, Alpha-2-macroglobulin, Complement, CD109, *Drosophila melanogaster*

INTRODUCTION

Epithelia form tissue barriers that separate functional compartments in organs. Occluding cell-cell junctions, which constrain the flow of solutes across the paracellular space, provide the epithelial diffusion barrier function. In vertebrates, tight junctions (TJs) form a seal between adjacent cells, thus providing a physical barrier that separates different membrane domains, restricts paracellular flux and

prevents pathogens from crossing epithelia (reviewed by Shin et al., 2006). In invertebrates, septate junctions (SJs) represent the functional equivalent of vertebrate TJs. SJs and TJs differ in their ultrastructure, subcellular localization and molecular composition. However, both types of occluding junctions contain four-transmembrane-domain proteins of the Claudin family at the core of the barrier-forming complex (Behr et al., 2003; Hemphälä et al., 2003; Paul et al., 2003). In vertebrates, the paranodal junctions between axons and glia cells (axo-glial septate junctions, or AGSJs) resemble the ultrastructure and molecular composition of invertebrate SJs, suggesting that SJs originated early during metazoan evolution and have been functionally conserved (Hortsch and Margolis, 2003; Banerjee et al., 2006). In invertebrates, SJs between glial cells provide the functional equivalent of the vertebrate blood-brain barrier (Carlson et al., 2000). Furthermore, SJs were shown to contribute to the immune barrier in the gut (Bonnay et al., 2013).

Although SJs and AGSJs have been intensely studied, many questions about their molecular components and their mechanism of assembly remain open. SJs are large multiprotein complexes containing cytoplasmic and integral membrane proteins, several of which were identified through genetic screens in *Drosophila* (reviewed by Wu and Beitel, 2004; Furuse and Tsukita, 2006; Banerjee et al., 2008). Two distinct subtypes of SJs are known: pleated SJs (pSJs) are found in ectodermal organs (epidermis, salivary glands, foregut, hindgut, tracheal system), whereas the ultrastructurally distinct smooth SJs (sSJs) form epithelial barriers in endodermal organs, such as the midgut (Tepass and Hartenstein, 1994). SJs are also essential for limiting the expansion of tracheal tubes during embryogenesis (Behr et al., 2003; Hemphälä et al., 2003; Paul et al., 2003), thus providing a phenotypic readout that enabled the identification of additional SJ components (Beitel and Krasnow, 2000). Interestingly, the barrier-forming and tube size-limiting functions of SJs are genetically separable, suggesting that SJs play multiple roles in epithelial morphogenesis and barrier formation (Paul et al., 2007). SJs are required for the accumulation of the secreted chitin deacetylases Serpentine (Serp) and Vermiform (Verm) in the tracheal lumen, where these proteins are required for limiting tube expansion, presumably through modifying a chitin matrix (Luschnig et al., 2006; Wang et al., 2006). In addition, SJ-associated basolateral polarity proteins of the Scribble (Scrib)/Discs large 1 (Dlg)/Lethal (2) giant larvae (Lgl) complex limit tracheal tube elongation by restricting Crumbs (Crb)-dependent apical membrane expansion (Laprise et al., 2010). Despite these advances, the precise role of SJs in tracheal tube size control is not clear yet. Furthermore, it is not known how the diverse functions of SJs are integrated and modulated in different tissues and under different physiological conditions. Recent genetic and proteomic studies suggest that many SJ-associated proteins remain to be identified

Institute of Molecular Life Sciences and PhD Program in Molecular Life Sciences, University of Zurich, Winterthurerstrasse 190, CH-8057 Zurich, Switzerland.
*Present address: Max Planck Institute of Neurobiology, Am Klopferspitz 18, D-82152 Martinsried, Germany.
[‡]These authors contributed equally to this work

[§]Author for correspondence (stefan.luschnig@imls.uzh.ch)

Development

(Hijazi et al., 2009; Nilton et al., 2010; Tiklová et al., 2010; Syed et al., 2011; Ile et al., 2012; Jaspers et al., 2012; Bonnay et al., 2013).

We identified Macroglobulin complement-related (Mcr) as a new SJ-associated protein. Mcr is a member of the widely conserved thioester protein (TEP) family, which includes α-2-macroglobulin (α2M) and complement proteins as key factors in innate immunity (Nonaka and Yoshizaki, 2004). These proteins contain a highly reactive intrachain thioester bond that mediates covalent binding to pathogen surfaces or to proteases. α2M, the most abundant serum protein in human blood, acts as an antiprotease that inactivates a broad spectrum of proteases. Upon proteolytic cleavage of a 'bait' region, α2M undergoes a conformational change and covalently binds the attacking protease to the exposed thioester (Borth, 1992). The α2M-protease complex is subsequently cleared by receptor-mediated endocytosis. Complement factors participate in opsonization of pathogens, targeting them for phagocytosis or lysis. Insect TEPs were first studied in *Drosophila melanogaster* and *Anopheles gambiae* and are involved in the response to pathogens and parasites, most notably *Plasmodium* (Lagueux et al., 2000; Levashina et al., 2001). *Drosophila* contains six TEP family members, four of which (Tep1-4) are predicted secreted proteins expressed in hemocytes and thought to play roles in innate immunity (Lagueux et al., 2000; Bou Aoun et al., 2011). *Tep5* appears to be a pseudogene in *Drosophila melanogaster* (Bou Aoun et al., 2011). Mcr (Tep6) is a diverged TEP family member with a mutated thioester motif and a predicted transmembrane domain not found in other TEPs, suggesting that the functions of Mcr are distinct from those of other TEPs. Mcr binds to the surface of *Candida albicans* cells and targets them for phagocytic uptake by cultured *Drosophila* S2 cells, thus resembling the opsonizing effect of α2M in vertebrates (Stroschein-Stevenson et al., 2006). However, it is not yet clear whether Mcr plays a similar role in pathogen clearance *in vivo*.

We report here a new and surprising role of Mcr in SJ-dependent epithelial barrier formation. We show that Mcr protein localizes to the lateral membranes of epithelial cells, where its distribution overlaps with known SJ components. Mcr is required in a cell-autonomous fashion for the correct localization of SJ components, indicating that membrane-bound rather than secreted Mcr isoforms are involved in SJ formation. Finally, *Mcr* is essential for SJ-dependent tracheal tube size control and epithelial barrier function. Our results, along with previous work (Stroschein-Stevenson et al., 2006), suggest that Mcr plays dual roles in epithelial barrier formation and innate immunity. These findings call attention to a potential link between pathogen defense mechanisms and the structure of occluding cell-cell junctions in epithelia.

RESULTS

A new gene required for tracheal tube length control

In a mutagenesis screen for genes involved in tracheal tube size control we isolated a complementation group with five lethal alleles showing overelongated tortuous tracheae (Fig. 1A,B; supplementary material Fig. S1). We named the locus *luftschlange* (*luf*). Four *luf* alleles (*luf^D13*, *luf^G249*, *luf^K101*, *luf^K103*) were embryonic lethal, whereas one allele (*luf^H25*) showed weaker tracheal phenotypes and was larval lethal. The amorphic allele *luf^K103* was used for most analyses. The tracheal dorsal trunk (DT) in stage 16 *luf^K103* embryos was 20% longer than that of controls (DT metameres 6-8; Fig. 1G). This effect was not due to an increase in tracheal cell number, which was unchanged in *luf* embryos (data not shown). Instead, the apical surfaces of DT cells in *luf* embryos were axially longer compared with controls, suggesting that abnormal cell shapes caused the overelongated tracheal phenotype in *luf* embryos (Fig. 1H,I). In
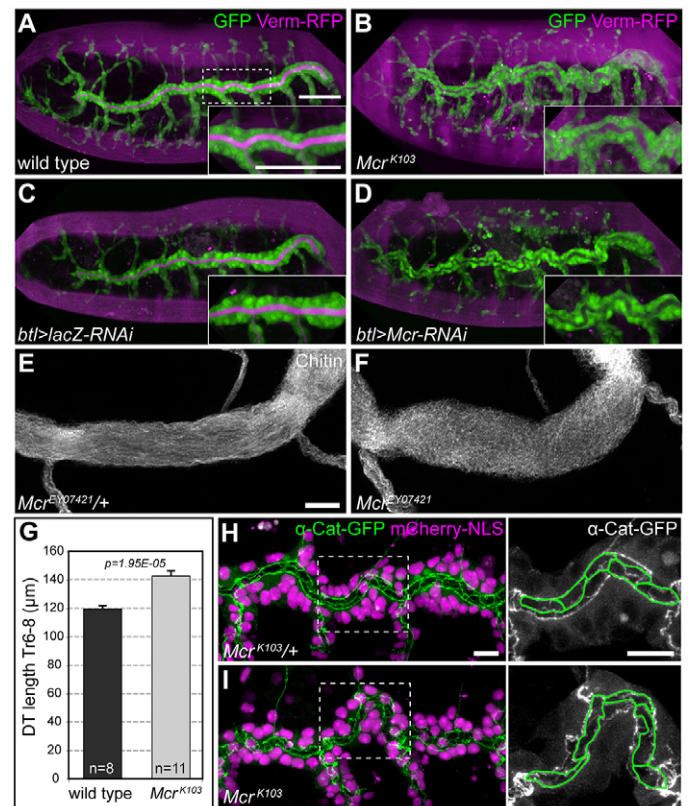

Fig. 1. Mcr is required to limit tracheal tube length and luminal protein accumulation. (A-D) Living stage 15 *Drosophila* embryos expressing cytoplasmic GFP (green) and secreted Verm-RFP (magenta) in tracheal cells controlled by *btl-Gal4*. *Mcr* mutations (B) or tracheal-specific expression of *Mcr* dsRNA (D) lead to overelongated tracheae compared with wild-type (A) or RNAi control (C) embryos. Note that Verm-RFP accumulates in tracheal lumina in wild-type and RNAi control embryos, whereas *Mcr* mutants and *Mcr* dsRNA-expressing embryos show reduced luminal Verm-RFP levels. Insets show magnifications of the boxed region in A. (E,F) Luminal chitin in fixed stage 15 embryos is organized into parallel fibrils in heterozygous *Mcr* control embryos (E), whereas the surface of the chitin cylinder is irregular and fibrils are disordered in *Mcr^EY07421* mutants (F). (G) Quantification of dorsal trunk luminal length in tracheal metameres 6-8 in wild-type and *Mcr^K103* mutant embryos. Error bars indicate s.e.m. (H,I) Tracheal metameres 6-8 in living stage 15 wild-type and *Mcr^K103* embryos expressing α-Cat-GFP and mCherry-NLS to label adherens junctions and nuclei in tracheal cells. Magnifications to the right show apical outlines of cells in metamere 7 highlighted in green. Note the abnormal elongation of apical cell surfaces along the tube axis in the *Mcr* mutant. DT, dorsal trunk. Scale bars: 50 μm in A-D; 5 μm in E,F; 10 μm in H,I.

addition, *luf* mutants showed markedly reduced levels of Verm-RFP protein in the tracheal lumen (Fig. 1B; supplementary material Fig. S1), although the total amount of Verm-RFP detectable in embryonic extracts by immunoblot was unchanged (supplementary material Fig. S2). Furthermore, luminal chitin fibrils, which run parallel to the tube axis in the wild type, appeared disordered in *luf* mutants (Fig. 1E,F). Altogether, the morphological defects in *luf* embryos were reminiscent of mutants lacking SJ components (Behr et al., 2003; Wu and Beitel, 2004; Wu et al., 2004; Wang et al., 2006).

luf is allelic to the *Mcr* locus

We mapped the *luf* locus to the cytological interval 28E1-E5. Within this interval, a lethal *P*-element insertion (*Mcr^EY07421*; Fig. 2A) (Bellen et al., 2004) in the 5′UTR of the *Mcr* gene failed to complement all five *luf* alleles. Embryos carrying *Mcr^EY07421* in *trans*
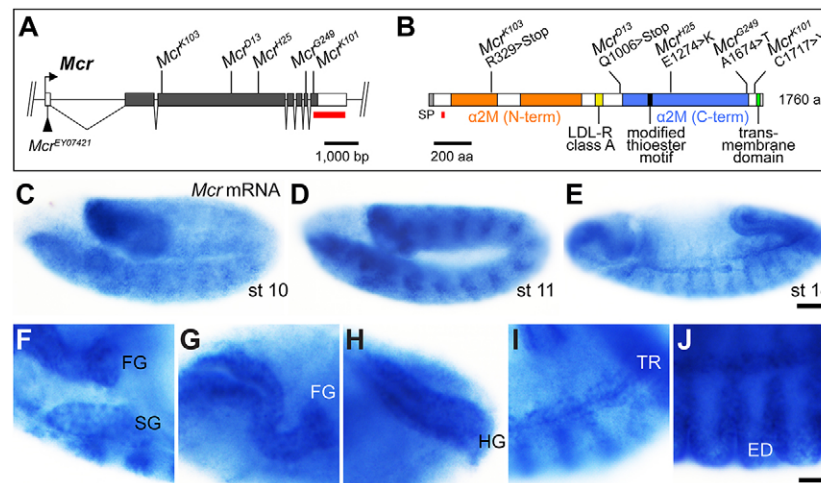
Fig. 2. *Mcr* is expressed in embryonic epithelial tissues. (A) Organization of the *Mcr* locus. Exons are shown as boxes with coding regions filled in black. Positions of EMS-induced mutations are indicated. *Mcr*[EY07421] is a *P*-element insertion in the 5′UTR of *Mcr*. The probe used for *in situ* hybridization is shown as a red bar. (B) Domain organization of Mcr protein. The signal peptide (SP), the N- and C-terminal α-2-macroglobulin (α2M) domains, the LDL receptor class A domain, the modified thioester motif, and the transmembrane domain are shown. *Mcr* mutations are indicated. The anti-Mcr antiserum (Stroschein-Stevenson et al., 2006) was raised against a peptide indicated by the red bar. (C) *In situ* hybridization with an *Mcr* antisense probe shows the embryonic expression pattern of *Mcr* mRNA. Developmental stage is indicated. Zygotic *Mcr* transcripts are first detectable at stage 10 in the hindgut and foregut regions. From stage 11 onwards, *Mcr* is expressed in salivary gland, tracheal and epidermal cells. Controls with a sense probe gave no comparable signals (data not shown). (F-J) Magnifications of stage 14 embryos showing *Mcr* expression in foregut (FG), salivary gland (SG), hindgut (HG), tracheal (TR) and epidermal (ED) cells. Scale bars: 50 μm in C-E; 20 μm in F-J.

to the *luf* alleles showed the *luf* tracheal phenotype (data not shown), indicating that *luf* is allelic to *Mcr*. Furthermore, tracheal-specific expression of *Mcr* dsRNA resulted in overelongated tubes resembling those associated with *luf* alleles (Fig. 1C,D). Together, these findings indicate that *Mcr* function is required in tracheal cells for limiting tube length and for luminal accumulation of Verm-RFP.

Mcr encodes a protein of 1760 amino acids with a predicted molecular weight of 203 kDa. It contains an N-terminal signal peptide sequence, a large extracellular part, a transmembrane domain, and a short cytoplasmic domain of 15 amino acids (Fig. 2B). The extracellular part resembles TEP/α2M family proteins with N- and C-terminal α-macroglobulin domains and a low-density lipoprotein receptor class A (LDLa) motif. The canonical thioester motif is mutated in Mcr, suggesting that Mcr does not function as a protease inhibitor (Stroschein-Stevenson et al., 2006; Bou Aoun et al., 2011). In addition, Mcr contains a predicted C-terminal transmembrane domain not found in other TEPs. The modified thioester motif and the transmembrane domain are conserved in insect Mcr/Tep6 homologs (Blandin and Levashina, 2004; Bou Aoun et al., 2011). Thus, Mcr represents a diverged member of the TEP family.

EMS-induced *Mcr* alleles carry point mutations affecting Mcr protein

Mcr[K103] and *Mcr*[D13] are amorphic alleles (data not shown) and contain premature stop codons predicted to result in truncated proteins of 329 and 1006 amino acids, respectively (Fig. 2A,B). Bands of the expected sizes (35 kDa and 130 kDa) were detectable in extracts from *Mcr*[K103] and *Mcr*[D13] embryos, respectively (supplementary material Fig S2). The remaining three alleles (*Mcr*[H25], *Mcr*[K101] and *Mcr*[G249]) carry missense mutations at residues that are conserved among insect Mcr/Tep6 homologs (Fig. 2B). The hypomorphic allele *Mcr*[H25] contains a glutamate-to-lysine exchange at position 1274 inside the α-macroglobulin complement component domain. *Mcr*[K101] contains a cysteine-to-tyrosine exchange at position 1717 N-terminal to the transmembrane domain. *Mcr*[G249] contains an

alanine-to-threonine exchange at position 1674 inside the α-macroglobulin receptor-binding domain. The amounts and electrophoretic mobility of Mcr proteins were unchanged in *Mcr*[H25], *Mcr*[K101] and *Mcr*[G249] embryos (supplementary material Fig. S2), suggesting that the missense mutations in these alleles affect Mcr protein function or localization.

Mcr is expressed in ectodermal epithelial tissues

We analyzed the expression pattern of *Mcr* mRNA during embryogenesis by *in situ* hybridization. *Mcr* mRNA was expressed in epithelial tissues from embryonic stage 10 [5 hours after egg lay (AEL)] onwards (Fig. 2C-E). *Mcr* transcripts were first detectable in the hindgut and epidermis and subsequently in the tracheal pits at stage 11 (9 hours AEL). During later embryonic stages, *Mcr* mRNA was found in the epidermis, tracheal system, foregut, hindgut and salivary glands (Fig. 2F-J), but not in the endodermal midgut. Thus, *Mcr* is selectively expressed in ectodermal epithelial tissues.

To study the distribution of Mcr protein we used an antiserum raised against a peptide located near the N-terminus after the signal sequence (Stroschein-Stevenson et al., 2006). On immunoblots, a band of ~210 kDa corresponding to full-length Mcr protein was detected throughout embryogenesis (supplementary material Fig. S3). This band was present in syncytial blastoderm embryos (0-1 hour AEL), indicating the presence of maternal *Mcr* gene products in the egg. Mcr protein levels increased during germ band extension (6 hours AEL) and continued to rise until the end of embryogenesis. As the levels of full-length Mcr protein increased, several bands of lower molecular weight appeared, which might represent degradation products or processed forms of Mcr protein (supplementary material Fig. S3).

Mcr protein localizes at the lateral plasma membrane of epithelial cells

Mcr protein was detectable in embryonic epithelia from germ band extension onwards (supplementary material Fig. S3). Mcr protein
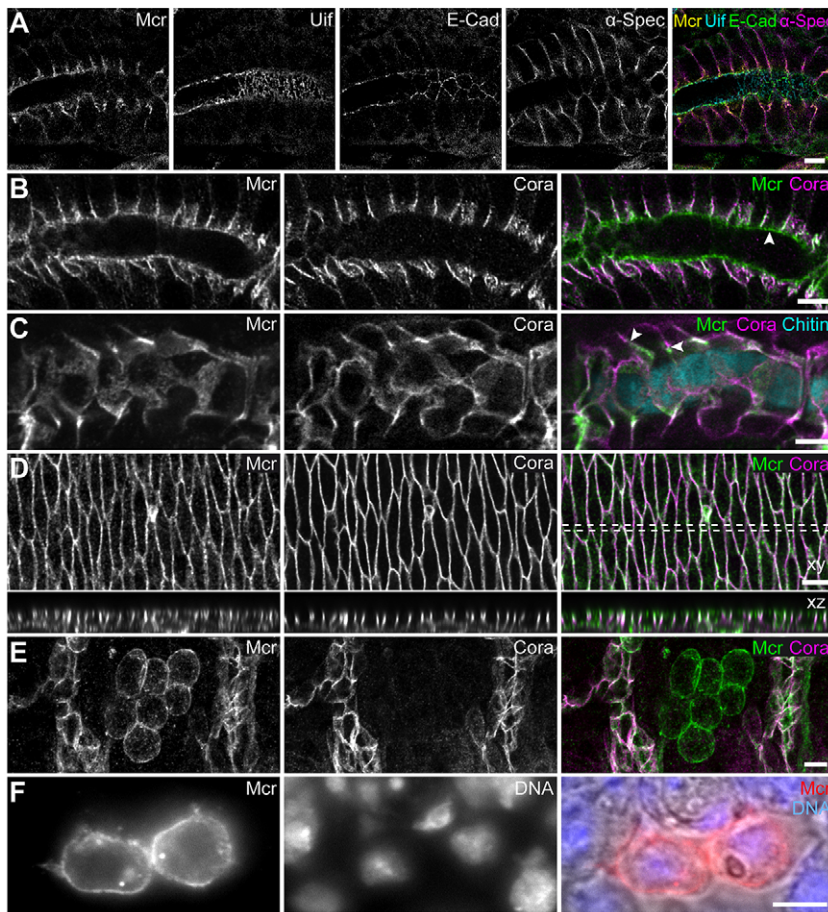
Fig. 3. Mcr protein localizes to lateral membranes of epithelial cells. (A) Confocal sections of embryonic stage 16 salivary glands immunostained for Mcr, Uninflated (Uif; apical membrane), E-Cadherin (E-Cad; adherens junctions) and alpha-Spectrin (α-Spec; Spectrin network below basolateral membrane). Mcr localizes to apicolateral and apical plasma membranes. (B-D) Confocal sections of stage 16 salivary gland (B), tracheal (C) and epidermal (D) cells immunostained for Mcr and Cora. Chitin (cyan) in C indicates the tracheal lumen. Mcr overlaps with Cora at lateral membranes, but extends further apically than Cora (arrowheads in C). Lower panels in D show an orthogonal transverse section of the boxed region in D. (E) Mcr localizes at germ cell membranes in embryonic gonads. Mcr- and Cora-expressing tracheal cells flank the gonad, which does not express Cora. (F) Mcr localizes to the plasma membrane and to intracellular puncta in transfected S2R+ cells expressing an *Mcr* cDNA. Note that Mcr protein is not detectable in non-transfected cells. Scale bars: 5 µm.

was enriched on lateral cell membranes of salivary gland, epidermis, tracheal and hindgut epithelial cells (Fig. 3). Double labeling with alpha-Spectrin to outline lateral cell boundaries indicated that Mcr levels are highest in the apical third of the lateral membrane (Fig. 3A). As this distribution was reminiscent of SJ components, we analyzed the localization of Mcr relative to SJ proteins. Mcr signals overlapped with the SJ-associated cytoplasmic ERM (Ezrin, Radixin and Moesin) protein Coracle (Cora) (Fehon et al., 1994) in salivary gland, epidermal and tracheal cells (Fig. 3B-D). However, in all cell types Mcr signals extended slightly further apically than Cora signals. In salivary glands, Mcr lined the apical cell surfaces facing the lumen, in addition to its distribution on lateral membranes (Fig. 3B). Mcr protein was also present on lateral cell membranes in larval imaginal discs, as well as in larval and adult trachea, foregut and hindgut, but not in the midgut and Malpighian tubules (data not shown). Interestingly, besides epithelial cells, we found Mcr protein also at the plasma membrane of embryonic germ cells and adult spermatocytes, which do not exhibit epithelial features such as SJs (Fig. 3E; data not shown). Consistent with previous work (Stroschein-Stevenson et al., 2006), we did not detect Mcr protein in cultured S2 cells. However, upon transient transfection of an *Mcr* cDNA, Mcr protein was detectable at the plasma membrane, as well as in intracellular puncta in S2 cells (Fig. 3F). Surprisingly, although *Mcr* is expressed in larval hemocytes (Bou Aoun et al., 2011), we were unable to detect *Mcr* transcripts and Mcr protein in embryonic hemocytes (data not shown). Taken together, Mcr is an unusual TEP that localizes to lateral membranes of ectodermal epithelial cells and to the plasma membrane of germ cells.

We analyzed the subcellular distribution of Mcr protein in the five mutant alleles in epidermis, salivary gland, hindgut, tracheal and germ cells (supplementary material Fig. S4). Mcr signals were abolished in Mcr^{K103} embryos and only residual signal was detectable in Mcr^{D13} embryos. By contrast, Mcr levels in the hypomorphic allele Mcr^{H25} and in the strong allele Mcr^{K101} were comparable to those of wild-type embryos. However, in both of these mutants Mcr protein was mislocalized basolaterally in salivary gland and hindgut cells. In Mcr^{G249} embryos, membrane localization of Mcr was lost and the protein instead accumulated intracellularly (supplementary material Fig. S4D). These findings suggest that correct membrane localization of Mcr protein, presumably mediated by the predicted transmembrane domain, is essential for Mcr function.

## Localization of SJ components depends on Mcr

The *Mcr* mutant phenotype and the localization of Mcr protein suggested that Mcr is involved in the assembly or maintenance of SJs. Mutations in SJ components lead to mislocalization of other SJ proteins and to breakdown of the entire complex (Ward et al., 1998; Genova and Fehon, 2003). We therefore examined the localization of the cytoplasmic SJ components Cora, Dlg (Woods and Bryant, 1991) and Scrib (Bilder and Perrimon, 2000) and of the membrane proteins Fasciclin III (FasIII) (Snow et al., 1989), Neurexin IV (Nrx-IV) (Baumgartner et al., 1996) and Neuroglian (Nrg) (Genova and Fehon, 2003) in salivary gland, tracheal, epidermal and hindgut cells of Mcr^{K103} embryos (Fig. 4; data not shown). The distribution of all SJ components tested was affected in *Mcr* embryos. The apicolateral accumulation of Cora and FasIII
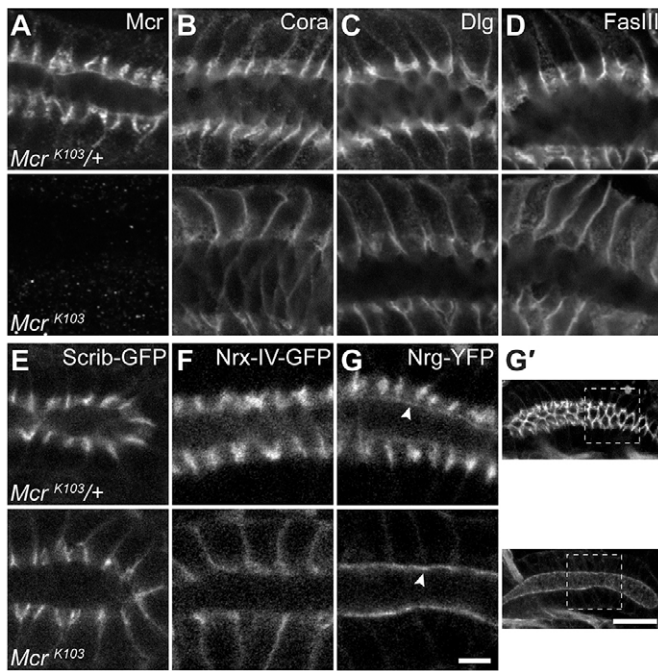
Fig. 4. Mcr is essential for the correct localization of SJ components.
(A-G) Confocal sections of salivary glands in fixed (A-D) and living (E-G) stage 15 embryos. In Mcr^{K103} heterozygous control embryos (upper rows), Cora (B), Dlg (C), FasIII (D), Scrib-GFP (E), Nrx-IV-GFP (F) and Nrg-YFP (G) are localized at the level of SJs in the apicolateral membrane. In Mcr^{K103} mutants (lower rows), in which Mcr protein is not detectable (A), the localization of Cora, Dlg, FasIII, Scrib-GFP and Nrx-IV-GFP extends basally and enrichment of these proteins at SJs is reduced or lost. Nrg-YFP is completely absent from lateral membranes in Mcr^{K103} embryos, whereas the apically localized pool (arrowheads) of Nrg-YFP increases in Mcr^{K103} mutants. (G′) Low-magnification projection of the salivary gland in G. Scale bars: 5 μm in A-G; 10 μm in G′.

was lost and the distribution of these proteins extended along the entire lateral membrane (Fig. 4B,D). Similarly, Dlg, Scrib-GFP and Nrx-IV-GFP were mislocalized basolaterally in Mcr^{K103} embryos, although these proteins were still partially enriched in the apicolateral zone (Fig. 4C,E,F). By contrast, Nrg-YFP was completely lost from lateral membranes of all epithelia in Mcr^{K103} embryos (Fig. 4G). Interestingly, a fraction of Nrg-YFP localizes at the apical membrane in wild-type salivary glands (Fig. 4G,G′). In Mcr mutants, this apical pool of Nrg-YFP appeared increased at the expense of basolateral Nrg-YFP, suggesting that Nrg-YFP redistributes in the absence of Mcr function and that Mcr is required to maintain Nrg at basolateral, but not at apical, membranes. Membrane localization of Nrg-YFP was rescued by the expression of a UAS-Mcr construct in epidermal stripes in Mcr mutant embryos (Fig. 5). Although the overexpressed Mcr protein was partially retained intracellularly, a fraction of the protein accumulated at the plasma membrane. Importantly, Mcr protein did not spread away from the producing cells (Fig. 5B) and Nrg-YFP membrane localization was restored only in the Mcr-expressing cells, but not in cells between the Mcr-expressing stripes (Fig. 5C), indicating that Mcr functions in a cell-autonomous manner to mediate Nrg membrane localization. Together, these findings suggest that Mcr acts cell-autonomously, presumably as an integral membrane protein, to recruit SJ components or to maintain their localization at the lateral membrane of epithelial cells.
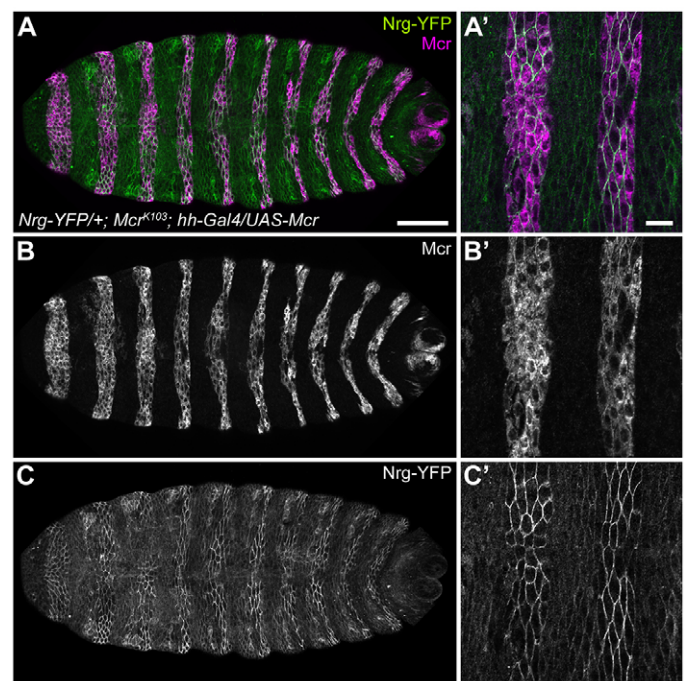

Fig. 5. Mcr functions cell-autonomously to mediate Neuroglian membrane localization. (A-C) Confocal section of Mcr^{K103} embryo expressing UAS-Mcr (B, magenta in A) in epidermal stripes controlled by hh-Gal4. Nrg-YFP (C, green in A) is expressed in all epidermal cells. Note that Mcr protein does not spread away from the hh-Gal4-expressing cells and that Nrg-YFP membrane localization is rescued in a cell-autonomous manner only in the Mcr-expressing cells. Scale bars: 50 μm in A-C; 10 μm in A′-C′.

SJ components are required for the correct localization of Mcr

We examined whether the localization of Mcr protein was also dependent on the presence of SJ components. We analyzed mutations in *megatrachea* (*mega*; *pickel* – FlyBase) (Behr et al., 2003), *sinuous* (*sinu*) (Wu et al., 2004), *Nrx-IV* and *Nrg* (Fig. 6; data not shown). Mutations in these core SJ components cause SJ protein mislocalization, loss of SJ structure and loss of barrier function. Cora was partially mislocalized basolaterally in $sinu^{06524}$ mutant salivary glands and hindguts (Fig. 6B′,F′) and uniformly mislocalized along lateral membranes in $Nrx-IV^{4304}$ and Nrg^{l7} salivary glands and hindguts (Fig. 6C′,D′,G′,H′). Similarly, the distribution of Mcr extended basolaterally in $sinu^{06524}$ and $Nrx-IV^{4304}$ mutant epithelia. However, Mcr protein remained partially enriched apicolaterally even in cells in which Cora was uniformly mislocalized (Fig. 6F,G), suggesting that Mcr might localize partially independently of Nrx-IV and Sinu. Strikingly, Mcr protein was strongly reduced in all epithelia in Nrg^{l7} mutant embryos, and residual Mcr protein localized to intracellular puncta (Fig. 6D,H; data not shown). Similarly, depletion of Nrg-YFP using anti-GFP nanobodies (Caussinus et al., 2011) in Nrg-YFP embryos caused loss of Mcr membrane staining in the nanobody-expressing cells (supplementary material Fig. S5). Thus, Mcr and Nrg mutually depend on each other for recruitment to, or maintenance at, the plasma membrane. Taken together, Mcr is required for the correct localization of SJ components and vice versa.

Mcr is required during SJ assembly

To test whether *Mcr* mutations affect the assembly or maintenance of SJs, we monitored the distribution of the cytoplasmic SJ protein
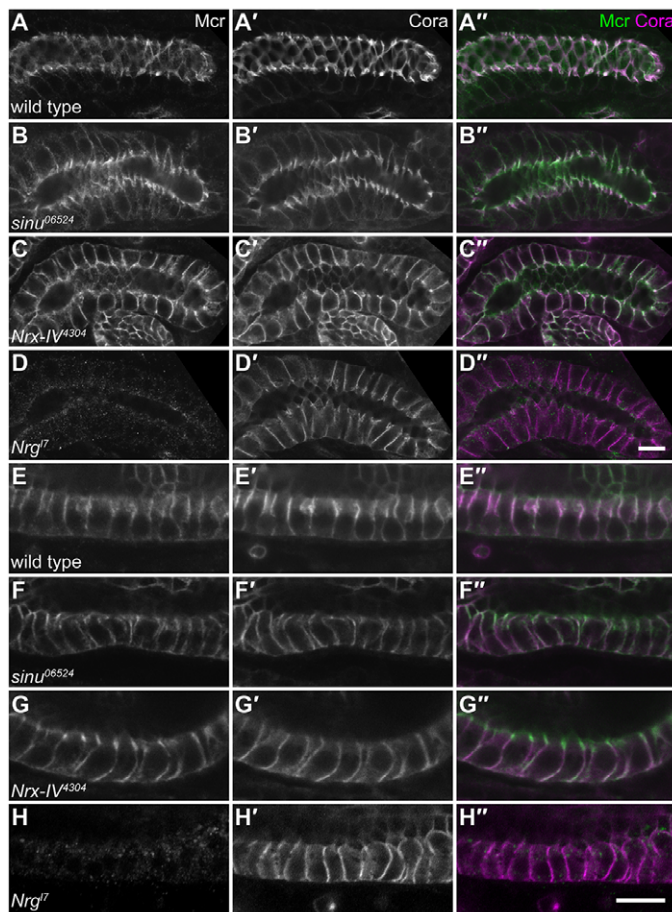
Fig. 6. The correct membrane localization of Mcr depends on SJ components. Immunostaining of Mcr (A-H, green in merge A″-H″) and Cora (A′-H′, magenta in merge) proteins in salivary glands (A-D) and hindguts (E-H) of stage 16 wild-type (A,E), *sinu^06524* (B,F), *Nrx-IV^4304* (C,G) and *Nrg^I7* (D,H) embryos. Cora is enriched at apicolateral membranes in the wild type, but extends basolaterally in *sinu^06524*, *Nrx-IV^4304* and *Nrg^I7* mutants. The distribution of Mcr extends basolaterally in *sinu^06524* and *Nrx-IV^4304* mutants, although Mcr remains partially enriched apically even in cells in which Cora is severely mislocalized (note the green apical Mcr signals in F″,G″). In *Nrg^I7* mutants, Mcr signals are dramatically reduced. Residual Mcr is detectable in intracellular puncta. Apical is up in E-H. Scale bars: 10 µm.

Cora and the integral membrane protein FasIII throughout SJ maturation in wild-type and in *Mcr^K103* embryos (Fig. 7). In wild-type hindgut epithelia, Cora starts to localize at apicolateral membranes at stage 14 and subsequently extends basally during SJ maturation (Fig. 7A). By contrast, *Mcr^K103* mutants show mislocalized Cora along the entire basolateral membrane from stage 14 (Fig. 7B). Similarly, FasIII was mislocalized from stage 14 in *Mcr^K103* embryos (Fig. 7C,D). Consistent with these findings, *Mcr* embryos lack pSJs in the hindgut and in other ectodermal epithelia (Fig. 7E,F; data not shown). Together, these results suggest that Mcr is required for the initial assembly of SJ complexes, in agreement with our finding that Mcr membrane accumulation precedes the onset of Cora expression during stage 13, when SJs first form in the epidermis (supplementary material Fig. S3) (Tepass and Hartenstein, 1994).

Mcr is essential for epithelial barrier function

Finally, we asked whether Mcr is required for SJ-dependent epithelial barrier function. We observed that the levels of secreted
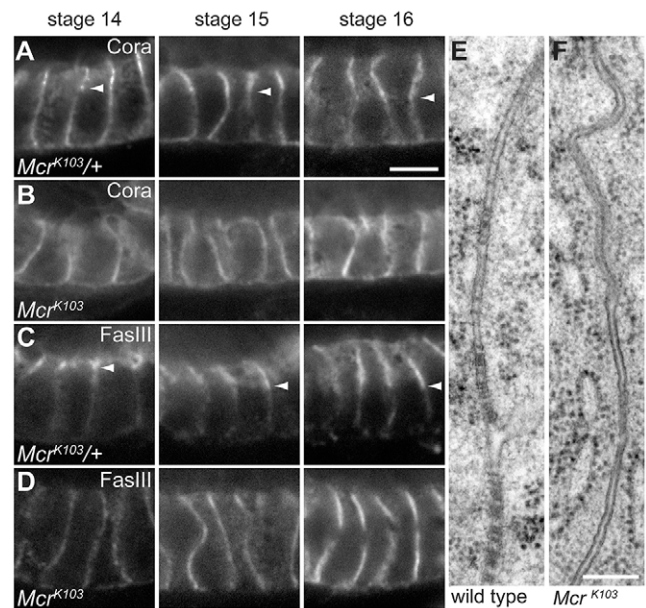

Fig. 7. Mcr is required during SJ assembly. (A-D) Confocal sections of embryonic hindguts stained for Cora (A,B) and FasIII (C,D). Apical is up in all panels. Embryonic stage is indicated. In *Mcr^K103*/+ heterozygous control embryos, Cora (A) and FasIII (C) localize at apicolateral membranes during stage 14 and continue to accumulate apicolaterally during subsequent stages (the basolateral front of accumulation is marked by arrowheads). In *Mcr^K103* mutants, Cora (B) and FasIII (D) are not restricted to the apicolateral prospective SJ region at stage 14 but are instead distributed throughout the lateral plasma membrane. This distribution persists during subsequent stages. (E,F) Transmission electron microscopy sections of apicolateral membranes in hindgut cells of stage 17 embryos. Note that the ladder-like septa corresponding to pSJs in the wild type (E) are absent in *Mcr^K103* mutants (F). Scale bars: 5 µm in A-D; 200 nm in E,F.

Serp-CBD-GFP protein in the tracheal lumen were reduced in *Mcr* embryos compared with controls. Instead, the protein became detectable in the hemocoel in *Mcr* mutants (Fig. 8A,B), suggesting that Serp-CBD-GFP is either not correctly secreted or that secreted Serp-CBD-GFP (33 kDa) is leaking across the tracheal epithelium. However, Serp-CBD-GFP did not accumulate inside tracheal cells in *Mcr* mutants (Fig. 8B), suggesting that the protein was not retained in the secretory pathway. We therefore probed epithelial barrier function in *Mcr* mutants by injecting Rhodamine-labeled dextran (10 kDa) into the hemocoel of stage 15 embryos (Lamb et al., 1998). In wild-type embryos fluorescent dextran was largely excluded from tracheal and hindgut lumina (Fig. 8C,E). By contrast, high levels of dextran were detectable inside the lumina of these organs in *Mcr^K103* embryos 20 minutes after injection (Fig. 8D,F), indicating that the epithelial barrier was defective. The phenotype of *Mcr^K103* embryos was comparable to that of *sinu* mutants, which lack functional SJs (Wu et al., 2004). Together, these results indicate that Mcr is essential for SJ-dependent epithelial barrier function. Leakage of luminal components, including Serp and Verm chitin deacetylases, across the tracheal epithelium might account for the tracheal tube size defects in *Mcr* mutants.

DISCUSSION

We describe a new and unexpected function of the complement-related protein Mcr in epithelial barrier formation. Insect TEPs are thought to function as secreted factors in innate immunity, although the functions of individual TEPs are not well understood (Blandin
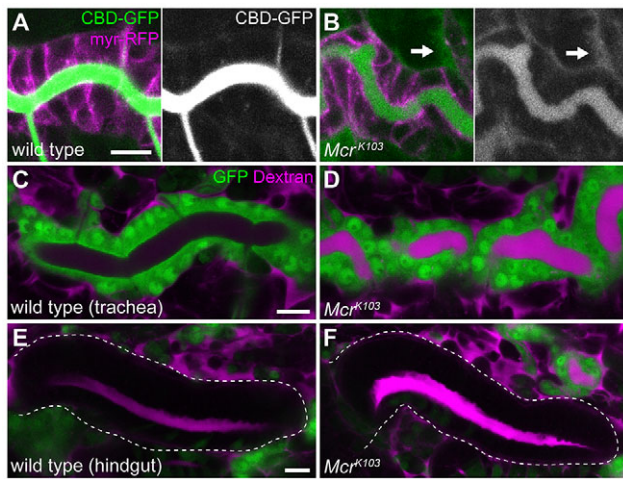
Fig. 8. *Mcr* is essential for epithelial barrier function. (A,B) Confocal sections of living stage 15 wild-type (A) and *Mcr*^{K103} mutant (B) embryos expressing Serp-CBD-GFP (CBD-GFP, green) in tracheal cells. Tracheal cell membranes are labeled by myristoylated RFP (myr-RFP, magenta). Note that luminal levels of Serp-CBD-GFP are lower in *Mcr* mutants than in the wild type. Conversely, Serp-CBD-GFP levels are elevated in the hemocoel (arrows in B) in *Mcr* mutants, suggesting that Serp-CBD-GFP is leaking across the tracheal epithelium in *Mcr* mutants. (C-F) Rhodamine-labeled 10 kDa dextran (magenta) was injected into stage 15 wild-type (C,E) and *Mcr*^{K103} mutant (D,F) embryos expressing GFP in tracheal cells (green). Dextran is largely excluded from the tracheal (C) and hindgut (E) lumen in wild-type embryos, but strongly accumulates 20 minutes after injection inside the lumen of *Mcr* mutant tracheae (D) and hindguts (F). The basal surface of the hindgut is outlined (dashed line in E,F). Scale bars: 10 μm.

and Levashina, 2004; Bou Aoun et al., 2011). We found that Mcr, a member of the diverged Tep6 subfamily, is a membrane-localized protein required for the assembly of SJs. This conclusion is based on three lines of evidence. First, we show that Mcr protein localizes at the lateral membrane of epithelial cells, where its distribution overlaps with that of known SJ components. Second, loss of *Mcr* function leads to morphological, ultrastructural and epithelial barrier defects resembling those of mutants lacking SJ components. This finding explains why mutations in *Mcr*, unlike other TEP genes, cause embryonic lethality (Bou Aoun et al., 2011). Third, Mcr is required in a cell-autonomous fashion for the correct assembly of SJ proteins at apicolateral membranes, and, conversely, SJ components are required for the correct membrane localization of Mcr.

Our finding that Mcr protein localizes at the plasma membrane and does not spread away from the producing cells suggests that full-length Mcr is an integral membrane protein, presumably anchored in the membrane by its predicted transmembrane domain. This notion is further substantiated by the recent mass spectrometry-based identification of Mcr along with several membrane-associated SJ proteins as components of the Claudin complex (Jaspers et al., 2012). However, earlier work had shown that Mcr is secreted by S2 cells into the culture medium (Stroschein-Stevenson et al., 2006). We were not able to detect secreted Mcr protein in the embryonic hemocoel or in tubular organ lumina, suggesting that the majority of Mcr protein is stably associated with the plasma membrane. However, secreted Mcr protein species might be present at low concentrations and may be poorly immobilized by chemical fixation, whereas the membrane-bound locally concentrated pool of the protein is readily detected by immunofluorescence. Consistent with this view, localized Mcr signals become visible only after the onset of zygotic *Mcr* expression, although Mcr protein of presumably

maternal origin is detectable by immunoblot throughout embryogenesis. These results and the presence of multiple Mcr-specific bands on immunoblots suggest that Mcr protein is processed into different cleavage products. Proteolytic cleavage may yield Mcr isoforms lacking the C-terminal transmembrane domain. Such Mcr cleavage products may be released from the plasma membrane through proteolytic shedding. Indeed, α2M proteins are proteolytically processed by attacking proteases, which are subsequently inhibited through covalent thioester bond formation with the α2M protein (Borth, 1992). The protease bait region is expected to render Mcr sensitive to protease cleavage, although attacking proteases are presumably not inactivated due to the mutated thioester motif. Thus, proteolytic processing of Mcr may result in multiple secreted and membrane-bound protein isoforms, which could carry out distinct functions. Secreted Mcr protein was shown to mediate opsonization of *C. albicans* cells and to promote their uptake by S2 cells in tissue culture (Stroschein-Stevenson et al., 2006). Secreted Mcr isoforms might play a similar role in pathogen clearance by hemocytes *in vivo*. Conversely, we show that membrane-localized Mcr is involved in SJ assembly and epithelial barrier function. Our finding that *Mcr* is required autonomously in tracheal cells suggests that integral membrane isoforms, rather than secreted Mcr protein, mediate tracheal tube size control and epithelial barrier function. However, these results do not formally exclude an autocrine requirement of secreted Mcr protein in tracheal cells.

The presence of Mcr in embryonic germ cells prompted us to test whether Mcr plays a role in gonad development. Although we did not detect defects in embryonic germ cell migration and gonad coalescence in zygotic *Mcr* mutants (data not shown), potential functions of *Mcr* in these processes might be masked by maternal *Mcr* gene products in the embryo. However, we found *Mcr* to be essential in the female germline for oogenesis, thus precluding the analysis of *Mcr* mutant germline clones.

The dynamics of SJ formation and the order of assembly of SJ components are not well understood. Our results suggest that Mcr plays an early role during SJ assembly at the lateral plasma membrane. Such a role is consistent with our finding that Mcr membrane accumulation precedes the accumulation of Cora at epidermal cell membranes. Mutations in all known SJ components cause mislocalization of all other components of the complex, indicating a high degree of mutual interdependence between SJ proteins (Ward et al., 1998; Oshima and Fehon, 2011). Similarly, we showed that Mcr is required for the correct localization of SJ components, and that Mcr localization depends on core SJ components. Furthermore, we found the immunoglobulin and fibronectin domain-containing transmembrane protein Nrg to be essential for maintaining membrane localization or stability of Mcr protein. Nrg might bind to the extracellular part of Mcr and thereby protect it from proteolytic cleavage. Alternatively, Nrg could be required at the transcriptional or translational level for Mcr expression. However, the abnormal punctate distribution of residual Mcr protein in *Nrg* mutants suggests that Nrg is required post-translationally, rather than for *Mcr* mRNA or protein synthesis. Although it is not yet clear whether Mcr and Nrg interact directly, the strict mutual dependency between the two proteins suggests that they act together to mediate an essential early step in SJ assembly. We speculate that Mcr might interact with other SJ-associated proteins, including Nrg, through its extracellular domain, because the small (15 amino acid) cytoplasmic domain of Mcr is not conserved among insects and lacks identifiable protein-binding motifs, such as the PDZ consensus binding sites that are found in several SJ components, including Gliotactin, Nrg, Nrx-

IV and the Claudins. The identification of binding partners of Mcr will be instrumental for understanding the molecular hierarchy of the SJ assembly pathway.

The discovery of a Macroglobulin complement-related protein as a component of SJs was surprising, since α2M proteins have generally been thought of as secreted factors involved in innate immunity, and functions of α2M as epithelial cell surface proteins have to our knowledge not been described thus far. *Anopheles* Tep1, which is the best-studied insect TEP, binds to bacteria and *Plasmodium* cells and targets them for phagocytosis (Levashina et al., 2001; Blandin and Levashina, 2004; Blandin et al., 2008). *Drosophila* Tep2 and Tep3 are required for phagocytosis by S2 cells of *E. coli* and *Staphylococcus aureus*, respectively, and Mcr is specifically required for phagocytosis of *C. albicans* (Stroschein-Stevenson et al., 2006). Our finding that Mcr is a cell surface protein required for epithelial barrier formation has potential implications for the evolution and function of occluding cell-cell junctions. SJs not only serve as a paracellular diffusion barrier, but they also prevent pathogens from crossing epithelial barriers and invading the organism. Mcr as a complement-like protein may therefore be strategically well placed on epithelial cell surfaces to provide a first line of defense against invading pathogens. This might be particularly relevant also for the gonads, where Mcr protein localizes on germ cell membranes. Interestingly, the process of pathogen encapsulation by hemocytes in insects involves the formation of SJ-like structures (Gupta and Han, 1988; Russo et al., 1996). Larger pathogens, such as parasitoid wasp eggs, are recognized by plasmatocytes and lamellocytes, which attach to and spread around the wasp egg, thus separating the pathogen from the hemocoel and enabling melanization of the capsule. This process involves the formation of an epithelial-like layer of multiple plasmatocytes surrounding the capsule (Russo et al., 1996). Interestingly, the encapsulating plasmatocytes are connected by SJs, which contain Cora and Nrg (Russo et al., 1996; Williams, 2009). Although this process has not been characterized in detail, it is likely that additional SJ components, possibly including Mcr, are involved in the formation of cell-cell junctions between immune cells. SJ-like structures were also observed between mammalian lymphocytes and macrophages upon encapsulation of pathogens (McIntyre et al., 1976; Siebert, 1979). These findings suggest an intriguing link between innate immunity and the formation of occluding cell-cell junctions. It is tempting to speculate whether mammalian CD109, a GPI-linked cell surface glycoprotein of the α2M family found on a subset of hematopoietic and myoepithelial cells (Hasegawa et al., 2007), might play similar roles to Mcr in *Drosophila*. Although the function of CD109 is largely unknown, it will be interesting to explore whether membrane-bound α2M proteins mediate functions in epithelial barrier formation and innate immunity in vertebrates and invertebrates.

MATERIALS AND METHODS
Drosophila strains and genetics
Fly stocks are described in FlyBase unless mentioned otherwise: w^1, *Abd-B-Gal4* 199 (de Navas et al., 2006), *btl-Gal4* (Shiga et al., 1996), *hh-Gal4*, *UAS-lacZ[RNAi]* (gift from Peter Gallant, University of Würzburg, Germany), *UAS-dicer2* (VDRC 60014), *UAS-Mcr[RNAi]* (VDRC 100197), *UAS-α-Cat-GFP* (Oda and Tsukita, 1999), *UAS-mCherry-NLS* (Caussinus et al., 2008), *UAS-Serp-CBD-GFP* (Luschnig et al., 2006), *UAS-myr-tdTomato* (Bloomington 32223), *UAS-NSlmb-vhhGFP4* (Caussinus et al., 2011), *Df(2L)Exel7034* (Bloomington 7807), *Mcr[EY07421]* (Bellen et al., 2004), *mega[G0012]* (Bloomington 11471), *Nrg[17]* (Bloomington 5595), *Nrx-IV[4304]* (Bloomington 4380), *sinu[06524]* (Bloomington 11690), *Scrib-GFP, Nrx-IV-GFP* (Buszczak et al., 2007) and *Nrg-YFP* (DGRC 115188). *Mcr* mutations

were induced by ethylmethanesulfonate (EMS) mutagenesis of a *btl-Gal4 UAS-GFP UAS-Verm-RFP* chromosome (Förster et al., 2010) and recombined onto FRT40A chromosomes. The *luf/Mcr* locus was mapped to 28E1-E5 by non-complementation of *Df(2L)Trf-C6R31* and *Df(2L)Exel7034* and by complementation of *Df(2L)TE29Aa-11*. For tracheal-specific RNAi, UAS-RNAi transgenes and UAS-*dicer2* were co-expressed using *btl*-Gal4.

Molecular biology
Genomic DNA was extracted from 20 homozygous *Mcr* embryos [identified by the absence of *CyO Dfd-YFP* (Le et al., 2006)] for each *Mcr* allele. The *Mcr* coding sequence, including exon-intron boundaries, was amplified from *Mcr* mutants and from the parental strain. PCR products were sequenced on both strands. UAS-Mcr was generated by amplifying the *Mcr* coding sequence from the *Mcr* full-length cDNA LD23292 (BDGP) using oligonucleotides (5′-3′, restriction sites are underlined): EcoRI-Mcr-F, ATAT<u>GAATTC</u>GAGCAATGATGTGGCACTTGC; and NotI-Mcr-R, TATA<u>GCGGCCGC</u>CCTGTGAGCAGTTGCATCATGT. The fragment was inserted between the *Eco*RI and *Not*I sites of pUASTattB (Bischof et al., 2007). The construct was integrated into the attP2 site at 68A4 using ΦC31 integrase (Bischof et al., 2007).

In situ hybridization
A 937 bp fragment containing the *Mcr* 3′UTR was amplified from genomic DNA using oligonucleotides containing the T7 RNA polymerase promoter either on the forward or reverse primer. PCR products were used as templates for *in vitro* transcription. Antisense and sense RNA probes were generated using digoxigenin-labeled UTP (Roche) and were detected using alkaline phosphatase-conjugated anti-digoxigenin Fab fragments (1:2000; Roche).

Immunofluorescence
Embryos were fixed in 4% formaldehyde in PBS/heptane for 20 minutes and devitellinized by shaking in methanol/heptane or ethanol/heptane (for anti-E-Cad immunostainings). The following antibodies were used: chicken anti-GFP (1:500; Abcam, ab13970), mouse anti-GFP (1:300; Clontech, JL8), rabbit anti-Mcr [1:1000; gift from A. Johnson, UCSF (Stroschein-Stevenson et al., 2006)], guinea pig anti-Cora [1:200 (Lamb et al., 1998)], mouse anti-Dlg (1:500; 4F3, DSHB), mouse anti-FasIII (1:50; 7G10, DSHB), mouse anti-alpha-Spec (1:50; 3A9, DSHB), guinea pig anti-Uif [1:1000 (Zhang and Ward, 2009)] and rat anti-DE-Cad (1:100; DCAD2, DSHB). Goat secondary antibodies were conjugated with Alexa 405, Alexa 488, Alexa 568 (Molecular Probes) or Cy5 (Jackson ImmunoResearch). Chitin was detected using Alexa Fluor-SNAP-tagged chitin-binding domain from *Bacillus circulans* chitinase A1, which was prepared as previously described (Caviglia and Luschnig, 2013).

Tissue culture
S2R+ cells were cultured on glass coverslips in Schneider's medium at 25°C. Cells were transfected with pUASTattB-Mcr using FuGene HD reagent (Promega). Forty-eight hours after transfection, cells were fixed with 4% formaldehyde/PBS and stained with anti-Mcr (Stroschein-Stevenson et al., 2006) and Hoechst 33342.

Light microscopy and image analysis
Imaging was performed using an Olympus FV1000 confocal microscope with 40×/1.3 NA and 60×/1.35 NA objectives. Images were processed using Huygens Deconvolution (SVI), ImageJ (v1.42), Imaris (v7.3.0; Bitplane) and Adobe Photoshop. For live imaging, embryos were dechorionated, mounted on glue-coated coverslips and covered with Voltalef 10S oil. The three-dimensional path of the DT lumen and apical cell outlines were traced using Imaris. Luminal length was measured in living embryos between fusion joints of DT metameres Tr5/6 and Tr8/9. *P*-values were calculated using Student's two-tailed, unpaired *t*-test.

Electron microscopy
Dechorionated stage 17 embryos were high-pressure frozen (Leica EM HPM100) and freeze-substituted (Leica EM AFS2) in 1% OsO₄ in water-free acetone. Subsequently, embryos were block-stained in 1% uranyl

acetate in water-free acetone for 1 hour at 4°C and embedded in Epon/Araldite (Sigma). Ultra-thin (50-70 nm) transverse sections of posterior abdominal segments were post-stained with lead citrate and imaged in an FEI Tecnai G2 Spirit transmission electron microscope.

Immunoblotting

Embryos were homogenized in Laemmli buffer. Equivalents of ten embryos per lane were loaded on 7.5% polyacrylamide SDS-PAGE gels. Proteins were transferred to nitrocellulose membranes by electroblotting. Membranes were probed with rabbit anti-Mcr [1:1000 (Stroschein-Stevenson et al., 2006)], mouse anti-α-Tubulin (1:50,000; Sigma, DM1A) and guinea pig anti-Verm [1:2500 (Wang et al., 2006)].

Dextran injections

Rhodamine-labeled 10 kDa dextran (Molecular Probes) was injected as described (Lamb et al., 1998) into wild-type and Mcr^{K103} embryos carrying *btl-Gal4 UAS-GFP*. Embryos were imaged 20 minutes after injection.

Supplementary material

Supplementary material available online at
http://dev.biologists.org/lookup/suppl/doi:10.1242/dev.102160/-/DC1

References

Banerjee, S., Sousa, A. D. and Bhat, M. A. (2006). Organization and function of septate junctions: an evolutionary perspective. *Cell Biochem. Biophys.* **46**, 65-77.

Banerjee, S., Bainton, R. J., Mayer, N., Beckstead, R. and Bhat, M. A. (2008). Septate junctions are required for ommatidial integrity and blood-eye barrier function in Drosophila. *Dev. Biol.* **317**, 585-599.

Baumgartner, S., Littleton, J. T., Broadie, K., Bhat, M. A., Harbecke, R., Lengyel, J. A., Chiquet-Ehrismann, R., Prokop, A. and Bellen, H. J. (1996). A Drosophila neurexin is required for septate junction and blood-nerve barrier formation and function. *Cell* **87**, 1059-1068.

Behr, M., Riedel, D. and Schuh, R. (2003). The claudin-like megatrachea is essential in septate junctions for the epithelial barrier function in Drosophila. *Dev. Cell* **5**, 611-620.

Beitel, G. J. and Krasnow, M. A. (2000). Genetic control of epithelial tube size in the Drosophila tracheal system. *Development* **127**, 3271-3282.

Bellen, H. J., Levis, R. W., Liao, G., He, Y., Carlson, J. W., Tsang, G., Evans-Holm, M., Hiesinger, P. R., Schulze, K. L., Rubin, G. M. et al. (2004). The BDGP gene disruption project: single transposon insertions associated with 40% of Drosophila genes. *Genetics* **167**, 761-781.

Bilder, D. and Perrimon, N. (2000). Localization of apical epithelial determinants by the basolateral PDZ protein Scribble. *Nature* **403**, 676-680.

Bischof, J., Maeda, R. K., Hediger, M., Karch, F. and Basler, K. (2007). An optimized transgenesis system for Drosophila using germ-line-specific phiC31 integrases. *Proc. Natl. Acad. Sci. USA* **104**, 3312-3317.

Blandin, S. and Levashina, E. A. (2004). Thioester-containing proteins and insect immunity. *Mol. Immunol.* **40**, 903-908.

Blandin, S. A., Marois, E. and Levashina, E. A. (2008). Antimalarial responses in Anopheles gambiae: from a complement-like protein to a complement-like pathway. *Cell Host Microbe* **3**, 364-374.

Bonnay, F., Cohen-Berros, E., Hoffmann, M., Kim, S. Y., Boulianne, G. L., Hoffmann, J. A., Matt, N. and Reichhart, J. M. (2013). big bang gene modulates gut immune tolerance in Drosophila. *Proc. Natl. Acad. Sci. USA* **110**, 2957-2962.

Borth, W. (1992). Alpha 2-macroglobulin, a multifunctional binding protein with targeting characteristics. *FASEB J.* **6**, 3345-3353.

Bou Aoun, R., Hetru, C., Troxler, L., Doucet, D., Ferrandon, D. and Matt, N. (2011). Analysis of thioester-containing proteins during the innate immune response of Drosophila melanogaster. *J. Innate Immun.* **3**, 52-64.

Buszczak, M., Paterno, S., Lighthouse, D., Bachman, J., Planck, J., Owen, S., Skora, A. D., Nystul, T. G., Ohlstein, B., Allen, A. et al. (2007). The carnegie protein trap library: a versatile tool for Drosophila developmental studies. *Genetics* **175**, 1505-1531.

Carlson, S. D., Juang, J. L., Hilgers, S. L. and Garment, M. B. (2000). Blood barriers of the insect. *Annu. Rev. Entomol.* **45**, 151-174.

Caussinus, E., Colombelli, J. and Affolter, M. (2008). Tip-cell migration controls stalk-cell intercalation during Drosophila tracheal tube elongation. *Curr. Biol.* **18**, 1727-1734.

Caussinus, E., Kanca, O. and Affolter, M. (2011). Fluorescent fusion protein knockout mediated by anti-GFP nanobody. *Nat. Struct. Mol. Biol.* **19**, 117-121.

Caviglia, S. and Luschnig, S. (2013). The ETS domain transcriptional repressor Anterior open inhibits MAP kinase and Wingless signaling to couple tracheal cell fate with branch identity. *Development* **140**, 1240-1249.

de Navas, L., Foronda, D., Suzanne, M. and Sánchez-Herrero, E. (2006). A simple and efficient method to identify replacements of P-lacZ by P-Gal4 lines allows obtaining Gal4 insertions in the bithorax complex of Drosophila. *Mech. Dev.* **123**, 860-867.

Fehon, R. G., Dawson, I. A. and Artavanis-Tsakonas, S. (1994). A Drosophila homologue of membrane-skeleton protein 4.1 is associated with septate junctions and is encoded by the coracle gene. *Development* **120**, 545-557.

Förster, D., Armbruster, K. and Luschnig, S. (2010). Sec24-dependent secretion drives cell-autonomous expansion of tracheal tubes in Drosophila. *Curr. Biol.* **20**, 62-68.

Furuse, M. and Tsukita, S. (2006). Claudins in occluding junctions of humans and flies. *Trends Cell Biol.* **16**, 181-188.

Genova, J. L. and Fehon, R. G. (2003). Neuroglian, Gliotactin, and the Na+/K+ ATPase are essential for septate junction function in Drosophila. *J. Cell Biol.* **161**, 979-989.

Gupta, A. P. and Han, S. S. (1988). Arthropod immune system. III. Septate junctions in the hemocytic capsule of the german cockroach, Blattella germanica. *Tissue Cell* **20**, 629-634.

Hasegawa, M., Hagiwara, S., Sato, T., Jijiwa, M., Murakumo, Y., Maeda, M., Moritani, S., Ichihara, S. and Takahashi, M. (2007). CD109, a new marker for myoepithelial cells of mammary, salivary, and lacrimal glands and prostate basal cells. *Pathol. Int.* **57**, 245-250.

Hemphälä, J., Uv, A., Cantera, R., Bray, S. and Samakovlis, C. (2003). Grainy head controls apical membrane growth and tube elongation in response to Branchless/FGF signalling. *Development* **130**, 249-258.

Hijazi, A., Masson, W., Augé, B., Waltzer, L., Haenlin, M. and Roch, F. (2009). boudin is required for septate junction organisation in Drosophila and codes for a diffusible protein of the Ly6 superfamily. *Development* **136**, 2199-2209.

Hortsch, M. and Margolis, B. (2003). Septate and paranodal junctions: kissing cousins. *Trends Cell Biol.* **13**, 557-561.

Ile, K. E., Tripathy, R., Goldfinger, V. and Renault, A. D. (2012). Wunen, a Drosophila lipid phosphate phosphatase, is required for septate junction-mediated barrier function. *Development* **139**, 2535-2546.

Jaspers, M. H., Nolde, K., Behr, M., Joo, S. H., Plessmann, U., Nikolov, M., Urlaub, H. and Schuh, R. (2012). The claudin Megatrachea protein complex. *J. Biol. Chem.* **287**, 36756-36765.

Lagueux, M., Perrodou, E., Levashina, E. A., Capovilla, M. and Hoffmann, J. A. (2000). Constitutive expression of a complement-like protein in toll and JAK gain-of-function mutants of Drosophila. *Proc. Natl. Acad. Sci. USA* **97**, 11427-11432.

Lamb, R. S., Ward, R. E., Schweizer, L. and Fehon, R. G. (1998). Drosophila coracle, a member of the protein 4.1 superfamily, has essential structural functions in the septate junctions and developmental functions in embryonic and adult epithelial cells. *Mol. Biol. Cell* **9**, 3505-3519.

Laprise, P., Paul, S. M., Boulanger, J., Robbins, R. M., Beitel, G. J. and Tepass, U. (2010). Epithelial polarity proteins regulate Drosophila tracheal tube size in parallel to the luminal matrix pathway. *Curr. Biol.* **20**, 55-61.

Le, T., Liang, Z., Patel, H., Yu, M. H., Sivasubramaniam, G., Slovitt, M., Tanentzapf, G., Mohanty, N., Paul, S. M., Wu, V. M. et al. (2006). A new family of Drosophila balancer chromosomes with a w- dfd-GMR yellow fluorescent protein marker. *Genetics* **174**, 2255-2257.

Levashina, E. A., Moita, L. F., Blandin, S., Vriend, G., Lagueux, M. and Kafatos, F. C. (2001). Conserved role of a complement-like protein in phagocytosis revealed by dsRNA knockout in cultured cells of the mosquito, Anopheles gambiae. *Cell* **104**, 709-718.

Luschnig, S., Bätz, T., Armbruster, K. and Krasnow, M. A. (2006). serpentine and vermiform encode matrix proteins with chitin binding and deacetylation domains that limit tracheal tube length in Drosophila. *Curr. Biol.* **16**, 186-194.

McIntyre, J. A., Pierce, C. W. and Karnovsky, M. J. (1976). The formation of septate-like junctional complexes between lymphoid cells in vitro. *J. Immunol.* **116**, 1582-1586.

Nilton, A., Oshima, K., Zare, F., Byri, S., Nannmark, U., Nyberg, K. G., Fehon, R. G. and Uv, A. E. (2010). Crooked, coiled and crimpled are three Ly6-like proteins

required for proper localization of septate junction components. *Development* **137**, 2427-2437.

Nonaka, M. and Yoshizaki, F. (2004). Evolution of the complement system. *Mol. Immunol.* **40**, 897-902.

Oda, H. and Tsukita, S. (1999). Dynamic features of adherens junctions during Drosophila embryonic epithelial morphogenesis revealed by a Dalpha-catenin-GFP fusion protein. *Dev. Genes Evol.* **209**, 218-225.

Oshima, K. and Fehon, R. G. (2011). Analysis of protein dynamics within the septate junction reveals a highly stable core protein complex that does not include the basolateral polarity protein Discs large. *J. Cell Sci.* **124**, 2861-2871.

Paul, S. M., Ternet, M., Salvaterra, P. M. and Beitel, G. J. (2003). The Na+/K+ ATPase is required for septate junction function and epithelial tube-size control in the Drosophila tracheal system. *Development* **130**, 4963-4974.

Paul, S. M., Palladino, M. J. and Beitel, G. J. (2007). A pump-independent function of the Na,K-ATPase is required for epithelial junction function and tracheal tube-size control. *Development* **134**, 147-155.

Russo, J., Dupas, S., Frey, F., Carton, Y. and Brehelin, M. (1996). Insect immunity: early events in the encapsulation process of parasitoid (Leptopilina boulardi) eggs in resistant and susceptible strains of Drosophila. *Parasitology* **112**, 135-142.

Shiga, Y., Tanaka-Matakatsu, M. and Hayashi, S. (1996). A nuclear GFP/ beta-galactosidase fusion protein as a marker for morphogenesis in living Drosophila. *Dev. Growth Differ.* **38**, 99-106.

Shin, K., Fogg, V. C. and Margolis, B. (2006). Tight junctions and cell polarity. *Annu. Rev. Cell Dev. Biol.* **22**, 207-235.

Siebert, A. E., Jr (1979). Septate-like junctions between cells of the immune system in vivo. *Cell Biol. Int. Rep.* **3**, 331-335.

Snow, P. M., Bieber, A. J. and Goodman, C. S. (1989). Fasciclin III: a novel homophilic adhesion molecule in Drosophila. *Cell* **59**, 313-323.

Stroschein-Stevenson, S. L., Foley, E., O'Farrell, P. H. and Johnson, A. D. (2006). Identification of Drosophila gene products required for phagocytosis of Candida albicans. *PLoS Biol.* **4**, e4.

Syed, M. H., Krudewig, A., Engelen, D., Stork, T. and Klämbt, C. (2011). The CD59 family member Leaky/Coiled is required for the establishment of the blood-brain barrier in Drosophila. *J. Neurosci.* **31**, 7876-7885.

Tepass, U. and Hartenstein, V. (1994). The development of cellular junctions in the Drosophila embryo. *Dev. Biol.* **161**, 563-596.

Tiklová, K., Senti, K. A., Wang, S., Gräslund, A. and Samakovlis, C. (2010). Epithelial septate junction assembly relies on melanotransferrin iron binding and endocytosis in Drosophila. *Nat. Cell Biol.* **12**, 1071-1077.

Wang, S., Jayaram, S. A., Hemphälä, J., Senti, K. A., Tsarouhas, V., Jin, H. and Samakovlis, C. (2006). Septate-junction-dependent luminal deposition of chitin deacetylases restricts tube elongation in the Drosophila trachea. *Curr. Biol.* **16**, 180-185.

Ward, R. E., IV, Lamb, R. S. and Fehon, R. G. (1998). A conserved functional domain of Drosophila coracle is required for localization at the septate junction and has membrane-organizing activity. *J. Cell Biol.* **140**, 1463-1473.

Williams, M. J. (2009). The Drosophila cell adhesion molecule Neuroglian regulates Lissencephaly-1 localisation in circulating immunosurveillance cells. *BMC Immunol.* **10**, 17.

Woods, D. F. and Bryant, P. J. (1991). The discs-large tumor suppressor gene of Drosophila encodes a guanylate kinase homolog localized at septate junctions. *Cell* **66**, 451-464.

Wu, V. M. and Beitel, G. J. (2004). A junctional problem of apical proportions: epithelial tube-size control by septate junctions in the Drosophila tracheal system. *Curr. Opin. Cell Biol.* **16**, 493-499.

Wu, V. M., Schulte, J., Hirschi, A., Tepass, U. and Beitel, G. J. (2004). Sinuous is a Drosophila claudin required for septate junction organization and epithelial tube size control. *J. Cell Biol.* **164**, 313-323.

Zhang, L. and Ward, R. E., IV (2009). uninflatable encodes a novel ectodermal apical surface protein required for tracheal inflation in Drosophila. *Dev. Biol.* **336**, 201-212.

Development